Article   **Open Access**

Evaluation of Geomechanical Properties for Tight Reservoir Using Uniaxial Compressive Test, Ultrasonic Test, and Well Logs Data

Nagham Jasim[1], Sameera M. Hamd-Allah[1], Hazim Abass[2]

[1] *Petroleum Engineering Department- Baghdad University, Iraq*
[2] *Halliburton and Colorado School of Mines, USA*

Abstract

Tight reservoirs have attracted the interest of the oil industry in recent years according to its significant impact on the global oil product. Several challenges are present when producing from these reservoirs due to its low to extra low permeability and very narrow pore throat radius. Development strategy selection for these reservoirs such as horizontal well placement, hydraulic fracture design, well completion, and smart production program, wellbore stability all need accurate characterizations of geomechanical parameters for these reservoirs. Geomechanical properties, including uniaxial compressive strength (UCS), static Young's modulus (E_s), and Poisson's ratio (u_s), were measured experimentally using both static and dynamic methods. Measured mechanical parameters on cores are used to correct well logs derived mechanical earth model (MEM). The analysis of measured mechanical properties of samples was conducted using the knowledge of cores mineralogy which was done in this study by the X-Ray Diffraction (XRD) test in addition to rock texture which was obtained using scanning electronic microscope (SEM). The study of SEM and TS of the samples explain the presence of vugges in some samples that cause its initial high porosity and consequently low UCS, also it causes lower compressional and shear velocity at these samples as compared to others. The minerals contained in each sample give a descriptive analysis of the difference of the values of both static and dynamic measured mechanical properties such as ultrasonic pulse traveling time, elastic properties, and UCS; this was explained through XRD results.

Keywords: *Mechanical properties, Uniaxial compressive test, Ultrasonic test, Mechanical earth model (MEM), X-ray diffraction(XRD), Scanning electronic microscope (SEM).*

1. Introduction

The uniaxial compressive strength (UCS), static Young's modulus (E_s), and Poisson's ratio (u_s) are the most crucial mechanical parameters of a formation. Prior knowledge of these parameters is very important in the applications oil industry. Mechanical properties of rocks are usually measured using two main techniques; destructive and non-destructive techniques. Destructive methods are conducted on a core sample to get simultaneously stress-strain relations and static mechanical properties are obtained from these curves. Non-destructive methods are dependent on the propagation of ultrasonic waves through the core samples for the determination of dynamic mechanical properties. The important step after the experimental measurement of mechanical properties is to find a transformation function that correlates static and dynamic elastic parameters. Mockovclakova and Pandula [1] studied the relation between static and dynamic moduli experimentally and they describe the insitu conditions where the measurements failed. Xu *et al.* [2] offered a geomechanical properties study of sandstone and shale samples; they established an empirical relation between static and dynamic elastic properties based on experimental results. Fie *et al.* [3] obtained static and dynamic parameters experimentally under different pressure and temperature conditions, also they find a correlation function between them and analyze the difference among them. Stimulation optimization of tight chalk was improved using a geomechanical evaluation study by

Salah *et al.* [4]. They correlated laboratory testing dynamic and static mechanical properties to well logs and used these parameters to calibrate the 1-D mechanical earth model. Elkatatny *et al.* [5] developed a direct correlation to estimate static Young's modulus from log data with the lacking of core measurements, where different reservoir types were used to match their correlation.

2. Mechanical properties measurements

2.1. Sample collection and preparation

S reservoir of Late Cretaceous age is located in the H oil field which field is located in the west of the Persian Gulf Basin and to the east of the Arabic Continental Shield. S formation was divided into 4 sub-layers according to the variation in lithology, electricity and petrophysical properties, which are: S-A, S-B1, S-B2 and S-B3. Sadi A only consists of mud lime but no hydrocarbon. S B1, S B2, Si B3 are of oil-bearing. All these formations are widespread in the H field. The evaluation indicates the thickness of each layer is: S A is about 51m; S B1 is 28m; S B2 is 30m; S B3 is 20m. Six core samples from the tight limestone S reservoir in the H oil field have been used for experimental measurement (Figure 1). These core samples are collected from two wells and cover the main three sections of the S reservoir (S-B1, S-B2, and S-B3). The depths, dimension, and petrophysical properties of the samples are listed in the Table 1. The selection of the core samples had three main considerations of availability of log data for the studied core sample depth (sonic- compressional and shear velocity, density, porosity), lateral distribution of cores with two wells, and cores from same well covering the main division of S- formation to capture variation in rock mechanical properties.

Table 1. Cores properties and dimensions

Wells	Sample no./fm.	Depth m	Length mm	Diameter mm	Bulk density gm/cc	Porosity %
Well B	1/S-B1	2673	50.70	38.15	2.67	18.73
	2/S-B2	2694	50.60	38.12	2.66	23.4
	3/S-B3	2711	50.76	38.15	2.68	24.58
Well C	4/S-B1	2735	50.90	38.60	2.66	15
	5/S-B2	2762	50.30	38.24	2.66	20.7
	6/Si-B3	2796	50.65	38.33	2.71	19.8

The prepared cores have the length to diameter (L/D) ratio of 2 to achieve the requirements of both ASTM D7012-14 [6] as well as the ASTM C597-02 [7] recommendation of a L/D ratio of 2-2.5 and 2-3, respectively. An electronic caliper is used to determine the length and diameter of the specimens. An average of two lengths measured parallel to each other from the center of the end faces is determined to the nearest 0.01 mm. The nearest 0.01 mm diameter is determined by taking the average of two diameters parallel to each other and close to the top, middle, and bottom of the core.

Figure 1. Tested core samples

2.2. Equipment system

2.2.1. Uniaxial compression test (UCT)

The UCT used in this study is of model ADR 1500; the system consists of a load frame with 2000 kN compression load, having a differential pressure transducer that keeps the actuator piston pressure difference on each. This transducer is calibrated to give the output force of the actuator, silent Flo Hydraulic Power Supply, axial extensometer with overall axial travel distance and a gauge length of 100.0 mm, and a circumferential extensometer.

2.2.2. Ultrasonic test

The experimental work was conducted with the ultrasonic pulsing method using the ultrasonic apparatus model ASTM C597-02. This instrument consists of A-Pulse generator, a pair of transducers (transmitter and receiver), amplifier, a circuit for time measuring, a unit for time display, and cables.

3. Testing procedure

Eighteen laboratory tests on 6 dry limestone core samples including unconfined compression tests, ultrasonic tests, and XRD tests were conducted according to the procedure suggested by ASTM D7012-14, and ASTM C597-02. The details of testing procedures are given in the following paragraphs.

3.1. Static method (uniaxial compression test)

The uniaxial compression tests were undertaken using (ADR 1500) testing equipment. This equipment can stratify the compressive load at a constant strain rate on the specimen with 2000 kN capacity. In this study, a strain rate equals to 0.25mm/mm/s was conducted at all compression tests. During the test, a pair of strain gauges were used to measure the applied load and resulted from deformation. The stress-strain data were continuously recorded and the stress at failure was considered as the UCS of the limestone core sample. The testing procedure that conforms with ASTM D7012-14 is summarized by raising the specimen to be in contact with the top platen then a small axial load, approximately100 N is applied to the core using the loading device to properly seat the bearing parts of the device, then starting recording the applied force, the resulted from axial and lateral deformations until sample breaks occur.

3.2. Dynamic method (ultrasonic test)

The accuracy of the experiment was ensured by checking and verifying the equipment to zero-time adjustment. This was done by applying coupling transducers and press them to the ends of the reference bar to get a stable transit time on the instrument screen. The zero references is reached if the appeared transit time is the same value marked on the bar. The P-Wave velocity is the measure of the time in m/s that the pressure wave takes to pass through a sample parallel to the wave direction. The S - Wave velocity is the time, in m/s, that the shear wave passes through the material in the direction of travel, which is perpendicular to particle motion. S - Waves travel slower through materials, providing a way to distinguish P from S Waves. Two piezoelectric transducers one acting as the transmitter and another as the receiver, are used to place the sample between them with suitable contact medium. The contact media used in the current test is a thin film of grease to achieve good transmission/reception of P and S-wave. According to the core's size, the frequencies of P and S-wave transducers are selected to be 200 kHz and 33 kHz, respectively. After the pulse traveling through the sample, the receiving transducer picked up it, and convert it to the electrical signal appear on the instrument screen. This signal gives both travel time in a microsecond and either compressional or shear velocities in m/s. The velocities of either P- or S-wave are estimated from the following relation:

$$V_p \text{ or } V_s \text{ (m/s)} = \frac{length\ of\ sample}{travel\ time} = \frac{s}{t} \quad\quad\quad (1)$$

where S is the distance traveled by the wave through the sample (mm); and t is the travel time (ms); V_P is the P-wave velocity (m/s); V_S is the S-wave velocity (m/s).

Spatial attention (using a microscope) should be taken before measuring to assure the absence of fractures or small holes on the core surface. Fractures or small holes in rock samples during testing will slow the waves down yielding faulty data.

4. Mechanical properties from laboratory results

4.1. Static mechanical properties

4.1.1. Uniaxial compressive strength (UCS)

The UCS of the cores is calculated using the following equation:

$$UCS = \frac{P}{A} \tag{2}$$

where P is the failure load (N); and A is the cross-sectional area (mm^2).

The obtained experimental stress- strain relation is used to find the ultimate uniaxial compressive strength (UCS), which is the peak value in the curve.

4.1.2. Elastic properties

The measured axial and lateral strain according to the corresponding applied force on the core sample is used to draw the stress-strain relation of each core sample which generally looks like Figure 2.

Axial and lateral strain ε_{axial}, $\varepsilon_{lateral}$ are calculated as follows:

$$\varepsilon_{axial} = \frac{change\ in\ sample\ length}{sample\ length} = \frac{\Delta L}{L} \tag{3}$$

$$\varepsilon_{lateral} = \frac{change\ in\ sample\ diameter}{sample\ diameter} = \frac{\Delta D}{D} \tag{4}$$

The Young's modulus, E is equal to the slope of the axial curve and the value of Poisson's ratio, υ, are calculated from the following equation (ASTM D7012-14):

$$\upsilon = -\frac{E}{slope\ of\ lateral\ curve} \tag{5}$$

The relation between the shear (G) and bulk (K) moduli and Young's modulus and Poisson's ratio are:

$$G = \frac{E}{2(1+\upsilon)} \tag{6}$$

$$K = \frac{E}{3(1-2\upsilon)} \tag{7}$$

4.1.3. Dynamic elastic properties

The dynamic Young's modulus and Poisson's ratio are calculated using the obtained v_p and v_s from ultrasonic test as follows:

$$u_d = \frac{VP^2 - 2VS^2}{2*(VP^2 - VS^2)} \tag{8}$$

$$E_d = \frac{\rho b\ VS^2 (3VP^2 - 4VS^2)^2}{2*(VP^2 - VS^2)} \ ... \tag{9}$$

where E_d=dynamic Young's modulus; ρ_b =density (g/cm^3); Vs=S-wave velocity (m/s); Vp=P-wave velocity (m/s), and υ= Poisson's ratio.

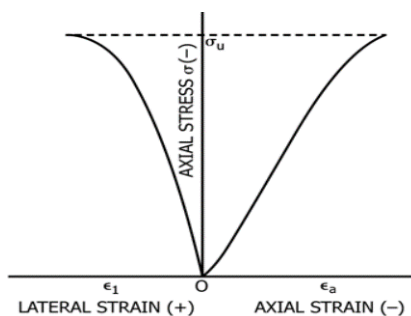## 5. Experimental work results

Figure 2. Lateral and axial strain stress relation

A data summary of the stress-strain results for the tested limestone core samples is included in Figs 3 through 8. These data have been used to calculate UCS, Poisson's ratio, and Young's modulus using the ASTM D7012-14 standard methods. The resulted mechanical properties of these samples are listed in the Table 2. Table 2 also shows the ultrasonic test results for the 6 core samples and the corresponding calculated dynamic elastic properties.

Table 2. Static and dynamic mechanical properties

Wells	Sample no./fm.	ρ_b, gm/cc	UCS, GPa	U_s	E_s, GPa	V_p, m/s	V_s, m/s	U_d	E_d, GPa
Well B	1/S-B1	2.67	73.509	0.330	19.98	3643.6	3149	0.25	15.568
	2/S-B2	2.67	57.871	0.257	17.23	3644	3148	0.25	19.099
	3/S-B3	2.68	52.402	0.157	5.406	3636	3143	0.25	14.129
Well C	4/S-B1	2.66	70.575	0.257	12.92	3400	2936	0.25	12.818
	5/S-B2	2.66	58.224	0.242	12.28	3402	2935.76	0.25	15.382
	6/S-B3	2.71	42.345	0.255	5.056	3392	2930	0.25	11.699
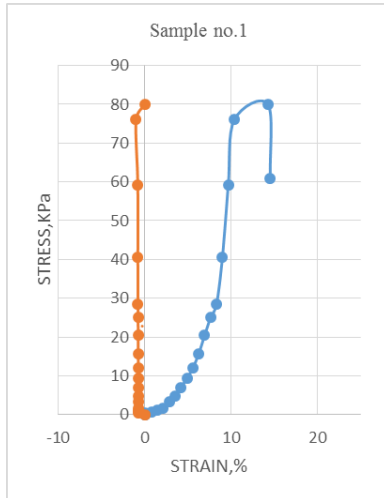
Figure 3. Stress-strain relation for sample no.1 S-B1
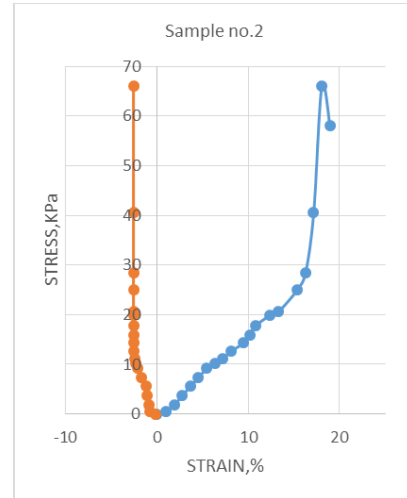
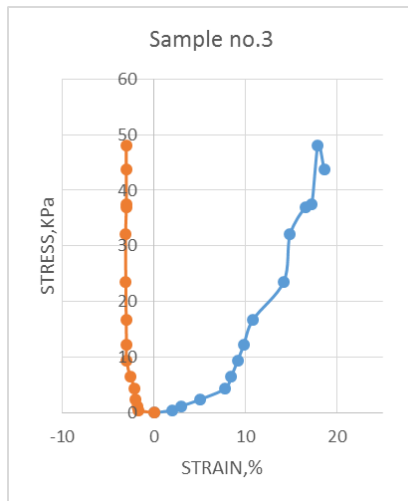Figure 4. Stress-strain relation for sample no.2.S-B2

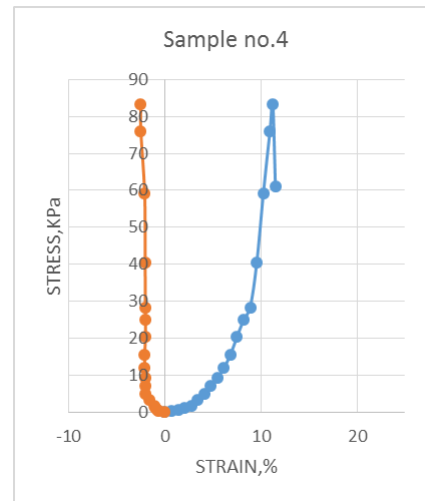

Figure 5. Stress-strain relation for sample no.3 S-B3

Figure 6. stress-strain relation for sample no.4 S-B1

6. Bulk density of the samples

The bulk density (ρ_b) is known as the mass per unit volume. It is equal to the mass of the dry core sample measured using sensitive balance divided by its bulk volume calculated using an electronic caliper. The measured bulk density of the studied core samples is listed in the Table 2.

7. X–Ray diffraction mineralogy test

Mineralogy is important in controlling the geomechanical properties of reservoirs. In order to measure or determine the mineralogical content of the samples, X – Ray Diffraction (XRD) was used to measure mineralogical percentages to support the results analyzing. Table 3 summarizes the results obtained by XRD. XRD was used to identify all the minerals present in the rock samples. Clay minerals were identified, which typically consist of Kaolinite, Illite and non-clay mineral such as Quartz in the sample. The results of the XRD test on the Table 3 illustrated in detail each of the quartz groups (including quartz and feldspars), the carbonate group (including calcite and dolomite), and the clay group (including total clays) and other minerals of rock samples.

Table 3. XRD test results of S formation

Wells	Sample no./fm.	Calcite, $CaCO_3$	Dolomite	k-feldspare	Na-feldspare	Pyrites, FeS_2	Quartz, SiO_2	Illite, K_2O	Chlorite,	Kaolinite	Total clay
Well B	1/ S-B1	87.6	0.5	0.5	0.144	0.00721	5.5	2.8	0.8	2.1	7.3
	2/ S-B2	83.8	1.8	0.078	0.165	0.0068	4.6	3.4	1	2.5	10.2
	3/ S-B3	89.3	1.5	0.11	0.23	0.04	5.9	1.7	1.7	5.3	15.2
Well C	4/ S-B1	89.9	0.4	0.104	0.286	0.064	4.56	2.74	0.524	1.4	4.56
	5/ S-B2	90	1.34	0.213	0.264	0.0091	4.24	3.33	0.798	1.403	7.43
	6/ S-B3	76.2	2.1	0.220	0.278	0.0355	5.18	2	1	1.87	17.1

8. Scanning Electron microscope (SEM) image

In geomechanical properties studies, the applications of SEM scanning is a direct approximation to examine the details of porous networks and the microstructural features by noticing full-diameter core sections to investigate the existence of fractures and vuges. The recognition of cracks distribution and geometry in the image is of very importance in elastic anisotropy data interpretation as well as the prediction of the rocks mechanical and hydraulic performance. Using of SEM is generally suitable for visualization from the meter to the millimeter. Microstructures for the tested core samples are discussed using SEM scanning image in Figure 9 through 14, which highlighted very important features that explain both strength and flow properties.
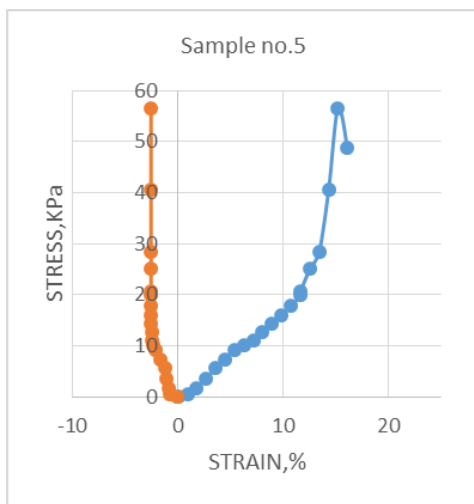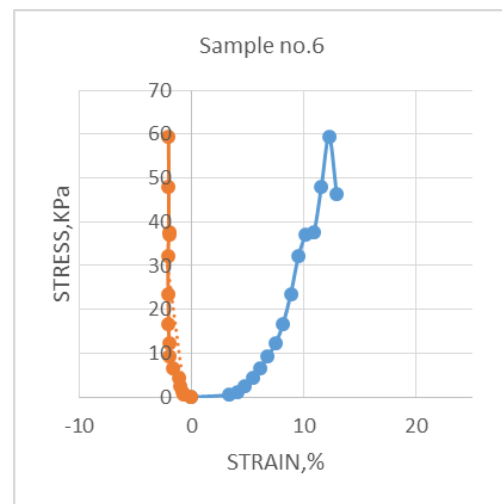

Figure 7. Stress-strain relation for sample no.5 S-B2   Figure 8. Stress-strain relation for sample no.6S-B3

Figures 9 and 10 are taken for S-B1 section samples no.1 and 4. SEM shows a micro crystalline limestone. Micro pores are associated with the micro crystalline matrix, that makes the porosity is not visible. Rigid grain increases significantly strengthen and stiffen of the sample and as such, give it more ability to support open fractures.

SEM shows a micro crystalline limestone. Micro pores are associated with the micro crystalline matrix, supported by vuggy pores, as shown in Figures 11 and 12 for S-B2 section samples no.2 and 5. Pores and vugges are relatively common in the micro crystalline parts of the two samples to indicate different microstructural pore features.
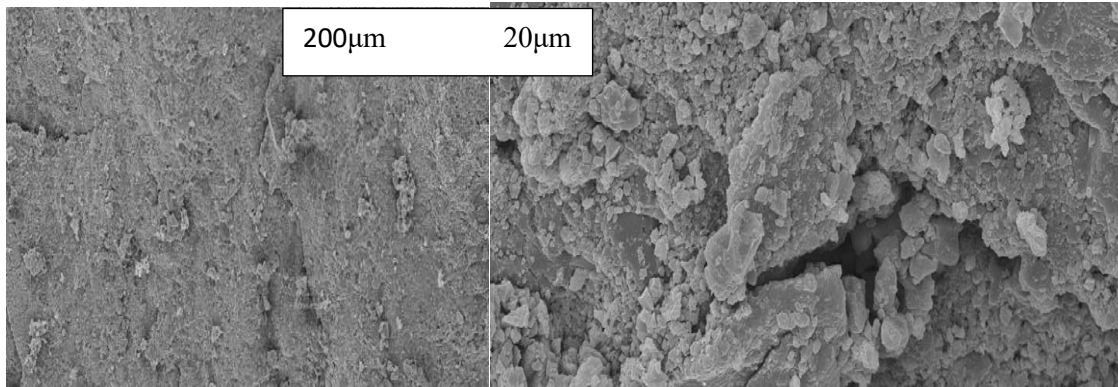
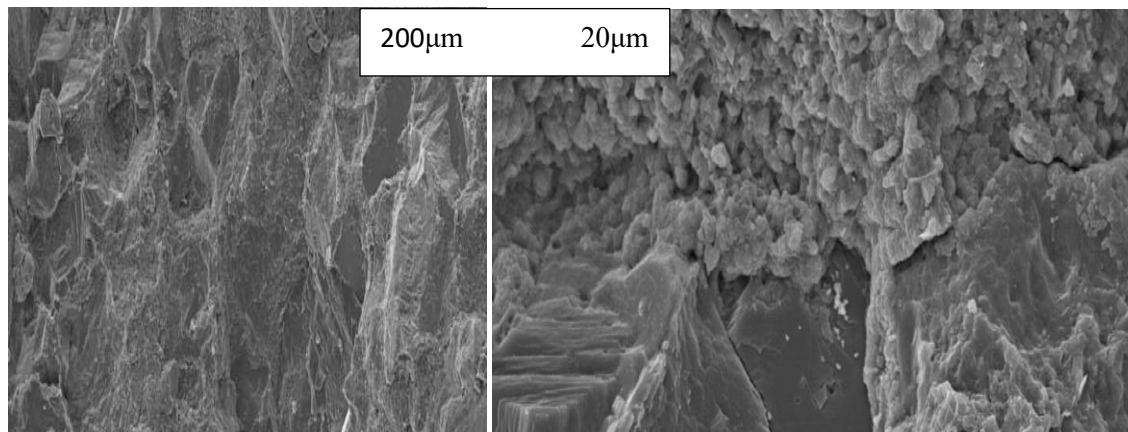

Figure 9. SEM image for sample no.1, S-B1
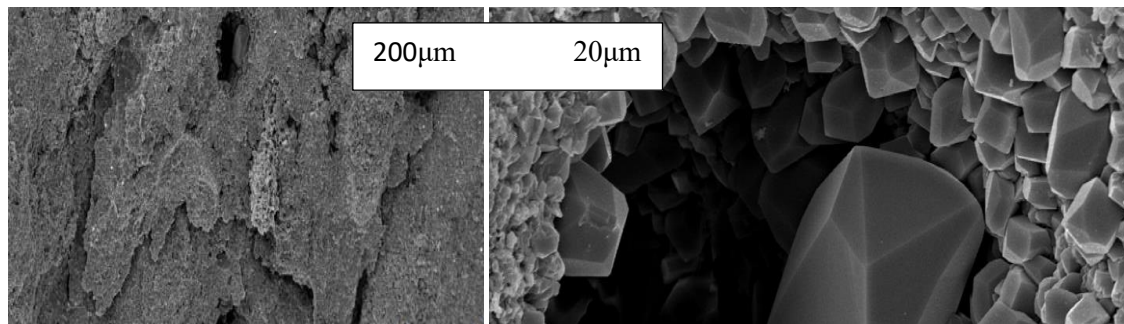

Figure 10. SEM image for sample no.4, S-B1
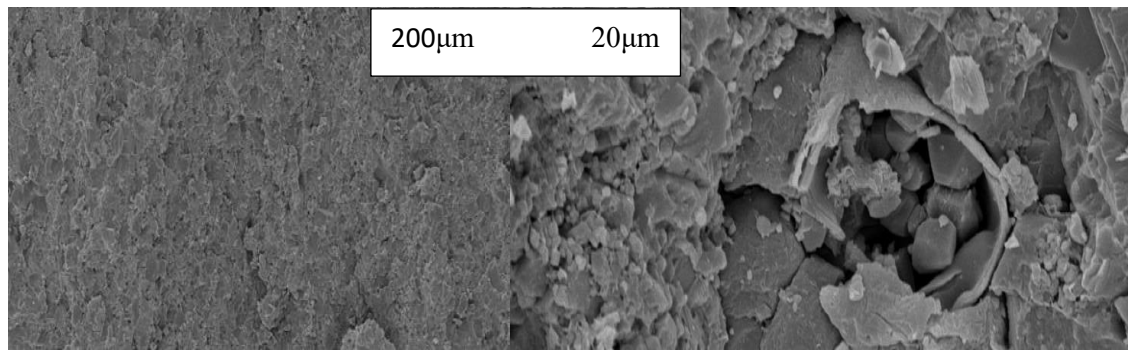

Figure 11. SEM image for sample no.2, S-B2.

200μm   20μm

Figure 12. SEM image for sample no.5, S-B2.
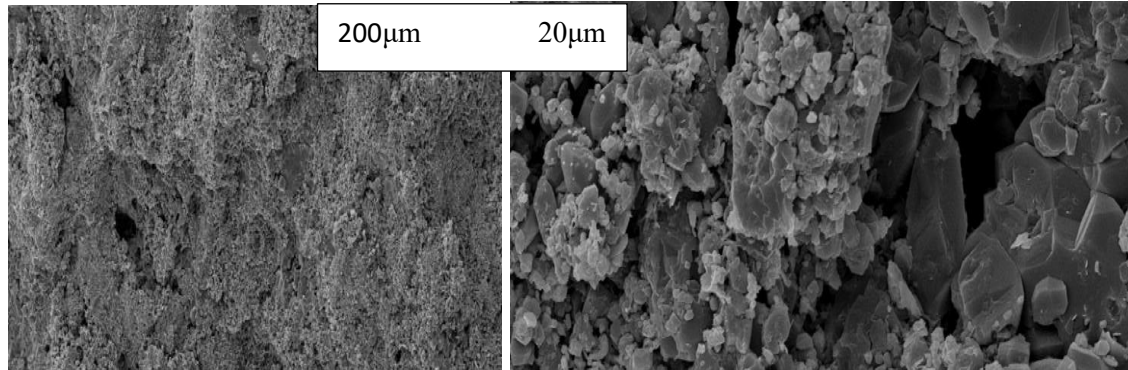

200μm   20μm

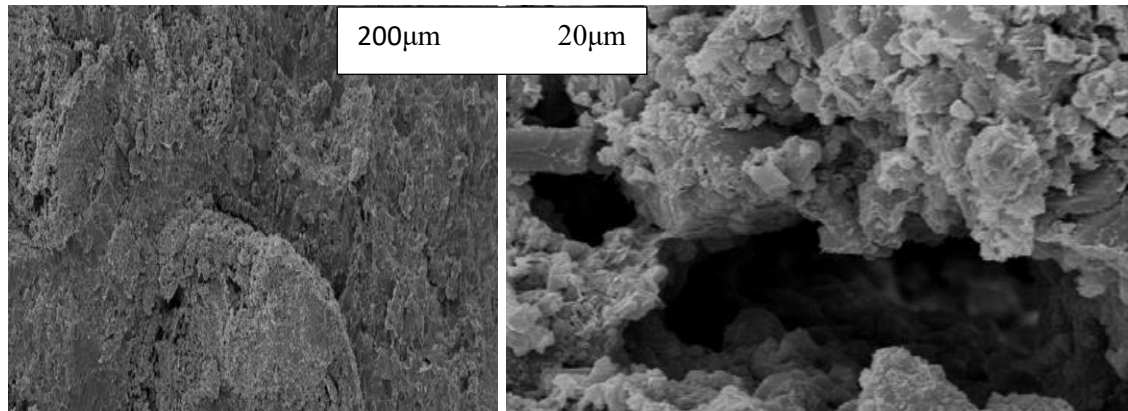Figure 13. SEM image for sample no.3, S-B3.

200μm   20μm

Figure 14. SEM image for sample no.6, S-B3.

S-B3 samples no.3 and 6 show a clay matrix supported the micro crystalline limestone matrix, micro pores surrounding more rigid grains and scattered vuggy pores are evolved in these samples. However, Figures 13 and 14 show a different micro fabric in the micro crystalline structure of this section.

9. 1-D MEM construction and correction

MEM represents the state of stress and rock mechanical properties for a certain stratigraphic section in the reservoir. The procedure to build the 1-D MEM model has been documented by many authors [11-12]. The poro-elastic horizontal strain model is used in MEM calculations. Mechanical rock properties are categorized into two groups; dynamic and statics. Dynamic mechanical properties calculations are based on sonic log (compressional Δt_{co} and shear Δt_s) and density log data, while static mechanical properties are estimated using empirical correlations [8-9]. Unconfined compressive strength (UCS), defined as the capacity of a rock to failure resistance, was estimated using the modified empirical equation of Chang [10]. For friction angle estimation, a correlation obtained from rock mechanics test data mentioned by

Sirat *et al.* [9], was used. Figures 15 and 16 display the output window representation of a MEM for both wells with the selected samples included in experimental work. The MEM includes critical data in tight reservoir development such as Young modulus (YME-DYN), Poisson's ratio (PR-DYN), unconfined compressive strength (UCS), vertical stress (σ_v), maximum horizontal stress (σ_H), and minimum horizontal stress (σ_h). Correction of MEM is a very important step in construction procedure; this step should be done using experimental mechanical properties measurement that has been summarized in Table 3. The illustration of corrected MEM for each well used in mechanical properties measurement is shown in Figure 15 and 16 by dots along with the depth interval of mechanical properties calculation. The difference between measured and calculated geomechanical properties are indicated in the Table 4.

Table 4. Difference between measured and log derived mechanical properties

Well	Geomechanical properties	Measured value	Calculated value
B	UCS, GPa	52.4-73.5	50-55
	υ	0.157-0.33	0.1-0.19
	E, GPa	5.4-19.92	10-35
	DT	274	80
	DTs	270	100-120
C	UCS, GPa	42.3-70.5	50-55
	υ	0.242-0.257	0.28-0.35
	E, GPa	5-12.9	10-40
	DT	290	100
	DTs	340	160-240

10. Analyzing laboratory results

The dynamic and static elastic mechanical properties of six core samples were measured in the same condition. The six samples have close values of bulk density, also the mineral composition of them illustrated in the Table 3 looks similar, the most important minerals which are related to geomechanical properties of the samples discussed here are the clay content minerals (illite and kaolinite). These minerals reflect samples hardness and indicate that S-B3 two samples have the largest clay content and consequently to be weaker than other samples with lower UCS, as listed in the Table 2.

SEM images shown in Figures 13 and 14 for the S-B3 two samples show the presence of vuggy pores to give an additional reason for low UCS of these samples and cause lower compressional and shear velocity as compared to other samples. The measured UCS of all samples gives a conclusion about the suitable layer among the three studied layers for the hydraulic fracturing stimulation technique.

It seems from the Table 2 that the dynamic Young's modulus is higher than the static Young's modulus in the same condition. There is a clear difference between the static and dynamic Poisson's ratio, the static Poisson's ratio distributes widely, while the dynamic Poisson's ratio differs slightly. The differences between the values of both static and dynamic parameters are affected by the situation of procedure under which the static and dynamic tests are conducted; such conditions like the values of applied strength are of several tents of KPa in static experiments, while the strength does not exceed the value of 100 Pa at dynamic methods. Also, at uniaxial tests, the applied loading can lead to the close of microcraks that cause the growth of deformation and consequently decrease the elastic constant. If we compare the two methods, no change in the structure of the material occurs in the non-destructive dynamic tests, which is the most important advantage of their use. The applying stress time set on the sample is also different between destructive and non-destructive methods; at static tests, it takes several minutes while at dynamic tests, it may take just microseconds that will not cause the closing of microcraks.
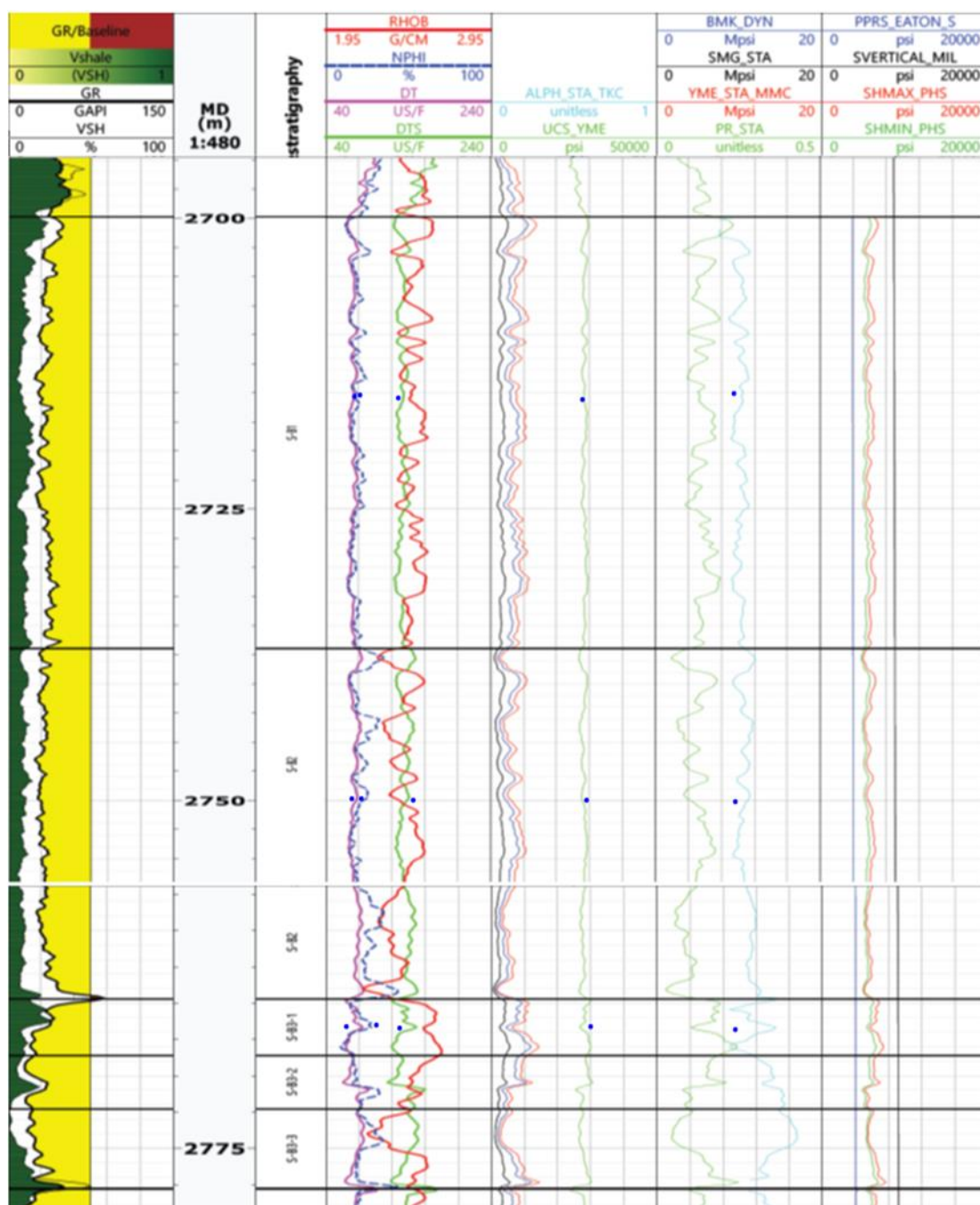
Fig. 15. Corrected MEM for measured data, well B

The velocity of ultrasonic pulses travelling in a solid material is affected by many factors such as density, porosity, texture, fluid content, and mineral composition. Well A samples have larger wave velocities as compared to those of well B caused by the more compact nature and higher bulk density of these samples. The type of minerals contained in each sample has a direct effect on elastic properties. The detailed mineralogy of the studied samples from XRD test showed that the samples contain various quantities of clay minerals (almost kaolinite) which have a clear effect in elastic properties so that as clay content increasing in S-B3 samples from the two studied wells leads to decreasing in grain bulk and shear modulus. These high Clay content samples are weaker of the other samples resulting in the low Young's modulus and weak strength parameters.
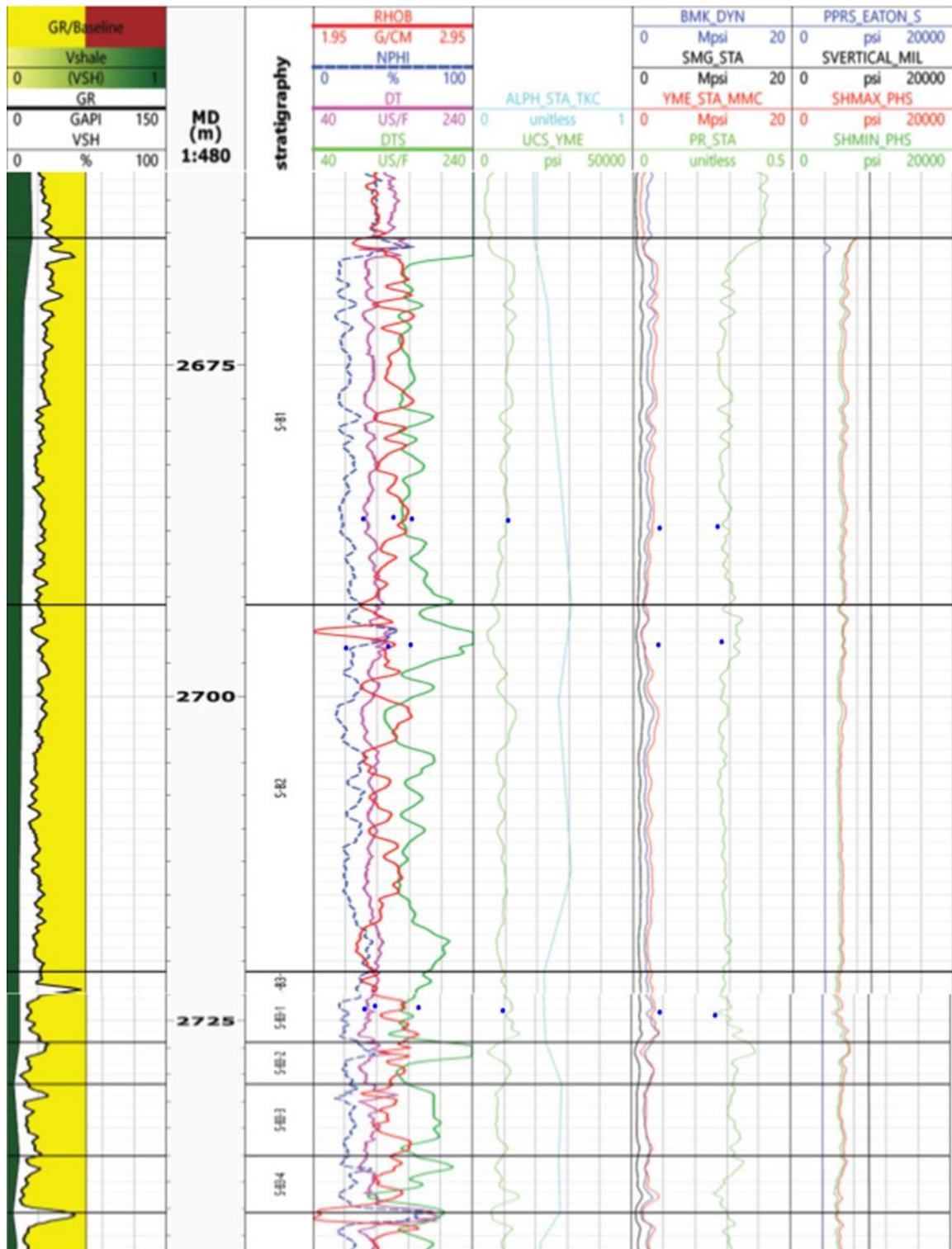
Fig. 16. Corrected MEM for measured data, well C

The measured geomechanical properties are then can be used to correct the calculated geomechanical properties and consequently reach to most accurate estimation of these properties to build mechanical earth model (MEM) which is a basic step in tight reservoir development strategy selection, including a sweet spot for horizontal well placement and hydraulic fracturing stage selection.

11. Conclusions

This paper focused on the measurement of both static and dynamic mechanical properties for a tight oil reservoir. The main conclusions that may be constructed from these results are:

- The procedure of measuring static and dynamic methods absolutely causes a clear difference between the measured property such as the initial load applied in the UCS method as compared with an ultrasonic method that causes to close the microcraks and deformation error estimation for the tested sample.
- The study of SEM and TS of the studied samples explain the presence of vugges in S-B3 samples that cause its initial high porosity and consequently low UCS of these samples and cause lower compressional and shear velocity as compared to other samples.
- The measured UCS of all samples gives a conclusion about the suitable layer among the three studied layers for the hydraulic fracturing stimulation technique.
- XRD test and the minerals contained in each sample give a descriptive analysis of the difference between static and dynamic measured mechanical properties such as ultrasonic pulse traveling time, elastic properties, and UCS of the samples.

Symbols

S	distance traveled by the wave through the sample (mm).
T	travel time (ms).
ε_{axial}, $\varepsilon_{lateral}$	axial and lateral strain.
L	sample length
D	sample diameter.
V_P	P-wave velocity (m/s).
V_S	S-wave velocity (m/s).
P	failure load (N).
A	cross-sectional area (mm^2).
E_d	dynamic Young's modulus.
ρ_b	density (g/cm^3).
Y	Poisson's ratio.
G	shear modulus.
K	Bulk modulus

References

[1] Mockovclakova A, and Pandula B. 2003. Study of the relation between the static and dynamic moduli of rocks. Institute of Geotechnics of Slovak Academy of Sciences.2003: 37-39.

[2] Xu H, Zhou W, Xie R, Da L, Xiao C, Shan Y, and Zhang H. Characterization of rock mechanical properties using lab tests and numerical interpretation model of well logs". Mathematical Problems in Engineering, 2016; (5):1-13.

[3] Fie W, Huiyuan B, Jun Y, and Yonghao Z.Correlation of dynamic and static elastic parameters of rocks. EJGE, 2016; 21: 1551-1560.

[4] Salah M, Petroleum K, Abdel-Maguid A, Crane B, Squires S, and Matzar L. Geomechanical evaluation enabled stimulation optimization of Apollonia tight chalk in Egypt", SPWLA 58thAnnual logging Symposium, June 17-21 2017.

[5] Elkatatny S, Mohamed M, Mohammed I, and Abdulraheem A. Development of a new correlation to determine the static Young's modulus. J Petrol Explor Prod Technol.,2018; 8: 17-30.

[6] ASTM, ASTM Annual Book of ASTM Standards, 2014, USA, ASTM D7012-14.

[7] ASTM, ASTM Annual Book of ASTM Standards, 2003, USA, ASTM C597-02.

[8] Fjaer E, Holt RM, Horsrud P, Raaen AM, and Risnes R. 1992. Petroleum Related Rock Mechanics, Elsevier 1992; vol. 53, 2nd edition.

[9] Sirat M, Ahmed M, and Zhang X. Predicting hydraulic fracturing in a carbonate gas reservoir in Abu Dhabi using 1D mechanical earth model: uncertainty and constraint. SPE-172942-MS.

[10] Chang C. Empirical rock strength logging in boreholes penetrating sedimentary formations. Chungnam National University, Daejeon, Geology and Earth Science, 2004; 7(3): 174–183.

[11] Plumb R, Edwards S, Pidcock G, and Lee D. The mechanical earth model concept and its application to high risk well construction projects. SPE 59128-MS, 2000.

[12] Ali A, Brown T, Delgado R. Watching rocks change- mechanical earth modeling. Oil Field Rev., 2003; 15 (1): 22-39.

To whom correspondence should be addressed: Nagham Jasim, Petroleum Engineering Department- Baghdad University, Iraq E-mail naghamjasim288@yahoo.com